THE JOURNAL OF BIOLOGICAL CHEMISTRY VOL. 284, NO. 42, pp. 28698–28703, October 16, 2009

Loss of TMEM16A Causes a Defect in Epithelial Ca^{2+}-dependent Chloride Transport*[S]

Received for publication, April 23, 2009, and in revised form, August 5, 2009 Published, JBC Papers in Press, August 13, 2009, DOI 10.1074/jbc.M109.012120

Jiraporn Ousingsawat[‡], Joana R. Martins[‡], Rainer Schreiber[‡], Jason R. Rock[§], Brian D. Harfe[§], and Karl Kunzelmann[‡1]

From the [‡]Institut für Physiologie, Universität Regensburg, Universitätsstrasse 31, D-93053 Regensburg, Germany and the [§]Department of Molecular Genetics and Microbiology, University of Florida, Gainesville, Florida 32610

Molecular identification of the Ca^{2+}-dependent chloride channel TMEM16A (ANO1) provided a fundamental step in understanding Ca^{2+}-dependent Cl^- secretion in epithelia. TMEM16A is an intrinsic constituent of Ca^{2+}-dependent Cl^- channels in cultured epithelia and may control salivary output, but its physiological role in native epithelial tissues remains largely obscure. Here, we demonstrate that Cl^- secretion in native epithelia activated by Ca^{2+}-dependent agonists is missing in mice lacking expression of TMEM16A. Ca^{2+}-dependent Cl^- transport was missing or largely reduced in isolated tracheal and colonic epithelia, as well as hepatocytes and acinar cells from pancreatic and submandibular glands of TMEM16A$^{-/-}$ animals. Measurement of particle transport on the surface of tracheas *ex vivo* indicated largely reduced mucociliary clearance in TMEM16A$^{-/-}$ mice. These results clearly demonstrate the broad physiological role of TMEM16A$^{-/-}$ for Ca^{2+}-dependent Cl^- secretion and provide the basis for novel treatments in cystic fibrosis, infectious diarrhea, and Sjöegren syndrome.

Electrolyte secretion in epithelial tissues is based on the major second messenger pathways cAMP and Ca^{2+}, which activate the cystic fibrosis transmembrane conductance regulator (CFTR)[2] Cl^- channels and Ca^{2+}-dependent Cl^- channels, respectively (1–3). CFTR conducts Cl^- in epithelial cells of airways, intestine, and the ducts of pancreas and sweat gland, while Ca^{2+}-dependent Cl^- channels secrete Cl^- in pancreatic acini and salivary and sweat glands (4–6). Controversy exists as to the contribution of these channels to Cl^- secretion in submucosal glands of airways and the relevance for cystic fibrosis (7–9). While cAMP-dependent Cl^- secretion by CFTR is well examined, detailed analysis of epithelial Ca^{2+}-dependent Cl^- secretion is hampered by the lack of a molecular counterpart. Although bestrophins may form Ca^{2+}-dependent Cl^- channels and facilitate Ca^{2+}-dependent Cl^- secretion in epithelial tissues (10, 11), they are unlikely to form secretory Cl^- channels in the apical cell membrane, because Ca^{2+}-dependent Cl^- secretion is still present in epithelia of mice lacking expression of bestrophin (12). Bestrophins may rather have an intracellular function by facilitating receptor mediated Ca^{2+} signaling and activation of membrane localized channels (13). With the discovery that TMEM16A produces Ca^{2+}-activated Cl^- currents with biophysical and pharmacological properties close to those in native epithelial tissues, these proteins are now very likely candidates for endogenous Ca^{2+}-dependent Cl^- channels (14–17). In cultured airway epithelial cells, small interfering RNA knockdown of endogenous TMEM16A largely reduced calcium-dependent chloride secretion (16). However, apart from preliminary studies of airways and salivary glands, the physiological significance of TMEM16A in native epithelia, particularly in glands, is unclear (14, 17).

MATERIALS AND METHODS

Animals and Ussing Chamber Experiments—Generation of a null allele of TMEM16a and TMEM16A knock-out animals has been described earlier (18). Mice (1–3 days) were sacrificed with Isofluran (Baxter, Germany). The pancreas and submandibular glands were removed, and epithelial cells were dispersed in a phosphate-buffered saline buffer composed of Collagenase VIII (Sigma, Taufkirchen, Germany). Tracheas were dissected, opened longitudinally on the opposite side of the cartilage-free zone, and transferred immediately into an ice-cold buffer solution. Stripped colon was put into ice-cold bath solution (145 mM NaCl, 0.4 mM KH_2PO_4, 1.6 mM K_2HPO_4, 6 mM D-glucose, 1 mM $MgCl_2$, and 1.3 mM calcium gluconate, pH 7.4) containing amiloride (10 μM) and indomethacin (10 μM). Experiments were performed as described previously (12).

Patch Clamp—Cells freshly isolated from mouse pancreatic and submandibular glands and liver were allowed to settle onto poly-L-lysine-coated cover slips. Patch clamp experiments were performed in the fast whole-cell configuration. Patch pipettes had an input resistance of 2–4 mega ohms, when filled with a solution containing 30 mM KCl, 95 mM potassium gluconate, 1.2 mM NaH_2PO_4, 4.8 mM Na_2HPO_4, 1 mM EGTA, 0.758 mM calcium gluconate, 1.034 mM $MgCl_2$, 5 mM D-glucose, and 3 mM ATP, pH 7.2. Ca^{2+} activity was 0.1 μM. We chose this solution because it avoids cell swelling, maintains the negative membrane voltage under whole-cell conditions, and enables proper hormone activation of Ca^{2+}-dependent ion currents (19). For some experiments, we removed K^+ from the pipette filling solution and replaced it with Na^+, to avoid contamination by K^+ currents. The access conductance was measured continuously and was 70–140 nanosiemens. The bath was perfused continuously at a rate of 10 ml/min with Ringer solution of the

* This work was supported by DFG SFB699, DFG KU 756/8-2, TargetScreen2 (EU-FP6-2005-LH-037365), and Else Kröner-Fresenius-Stiftung P36/05//A44/05.

[S] The on-line version of this article (available at http://www.jbc.org) contains supplemental Figs. 1 and 2.

[1] To whom correspondence should be addressed. Tel.: 49-0-941-943-4302; Fax: 49-0-941-943-4315; E-mail: karl.kunzelmann@vkl.uni-regensburg.de.

[2] The abbreviations used are: CFTR, cystic fibrosis transmembrane conductance regulator; CCH, carbachol; wt, wild type.

following composition: 145 mM NaCl, 0.4 mM KH_2PO_4, 1.6 mM K_2HPO_4, 6 mM D-glucose, 1 mM $MgCl_2$, and 1.3 mM calcium gluconate, pH 7.4). All experiments were performed at 37 °C. Currents (voltage clamp) and voltages (current clamp) were recorded using a patch clamp amplifier (EPC 7, List Medical Electronics, Darmstadt, Germany), the LIH1600 interface and PULSE software (HEKA, Lambrecht, Germany) as well as Chart software (ADInstruments, Spechbach, Germany). Data were stored continuously on a computer hard disc and were analyzed using PULSE software. In regular intervals, membrane voltages (V_c) were clamped in steps of 10 mV from −50 to +50 mV relative to resting potential. In some experiments, cells were voltage clamped over a larger voltage range. Membrane conductance G_m was calculated from the measured current (I) and V_c values according to Ohm's law. Membrane conductances were measured in the current clamp mode of the amplifier.

Measurement of Mucociliary Clearance—Tracheas were prepared as for Ussing chamber recordings. Tracheas isolated from mice were mounted with insect needles onto extra thick blot paper (Bio-Rad) and transferred into a water-saturated chamber at 37 °C. The filter paper was perfused with Ringer solution at a rate of 1 ml/min and at 37 °C. Polystyrene black-dyed microspheres (diameter 6.51 ± 0.58 μm, Polybead®, Polyscience Inc., Warrington, PA) were washed with Ringer solution and ~10 μl of particle solution with ~0.5% latex were added onto the mucosal surface of the trachea. Particle transport on different conditions was visualized by images every 10 s for 15 min using a Zeiss stereo microscope Discovery version 12, with digital camera AxioCam ICc1 and AxioVision software (Zeiss, Göttingen, Germany). Particle speed was calculated using AxioVision software (release 4.6.3, Zeiss).

In Situ Hybridization—Tissues were harvested from wild type 3-day-old mice and fixed overnight in 4% paraformaldehyde in phosphate-buffered saline. After cryoprotection in 30% sucrose, tissues were frozen (Sakura, Torrance, CA). 14-μm cryosections were hydrolyzed in 0.2 N HCl, permeabilized in 3 μg/ml proteinase K, fixed again in 4% paraformaldehyde, and acetylated in 0.25% acetic acid before hybridization with a digoxigenin-labeled Tmem16a riboprobe overnight at 65 °C as described previously. After washes in saline-sodium citrate, digoxigenin was detected using an alkaline phosphatate-conjugated anti- digoxigenin antibody (Roche, 1:2,000) and 5-bromo-4-chloro-3-indolyl phosphate/nitro blue tetrazolium substrates (Sigma).

Materials and Statistical Analysis—All chemicals (ATP, UTP, carbachol, CFTRinh-172, isobutylmethylxanthine, forskolin, and 4,4′-diisothio-cyanostilbene-2,2′-disulfonic acid (DIDS)) were from Sigma (Taufkirchen, Germany) or Merck (Darmstadt, Germany). The anti-human TMEM16A was a generous gift from Professor van de Rijn (Department of Pathology, Stanford University. (Student's t test (for paired or unpaired samples as appropriate) and analysis of variance was used for statistical analysis.) $p < 0.05$ was accepted as significant.

RESULTS AND DISCUSSION

Defective Ca^{2+}-dependent Cl^- Secretion in Airways of $TMEM16A^{-/-}$ Animals—We examined Ca^{2+}-dependent Cl^- secretion in epithelial tissues from wild type (wt) mice and from mice lacking expression of TMEM16A. As reported earlier, knock-out of TMEM16A in mice leads to death within one month of birth (18). Utilizing a micro Ussing chamber that allows measurements of the transepithelial voltage (V_{te}) in tracheas from 3–5 day old mice, we examined Ca^{2+}-dependent Cl^- secretion upon stimulation with the muscarinic M3 receptor agonist carbachol (CCH) (20). Basolateral application of CCH induced a negative voltage deflection, indicating activation of transient Cl^- secretion, probably by submucosal glands of tracheas from $TMEM16A^{+/+}$ mice (Fig. 1, *A* and *B*). Cl^- secretion was inhibited by niflumic acid and by Ca^{2+} depletion from the endoplasmic reticulum, using the Ca^{2+}-pump inhibitor cyclopiazonic acid (Fig. 2, *A* and *B*). Thus, Ca^{2+}-dependent Cl^- secretion in murine neonatal tracheas is similar to that in adult tracheas but of much smaller amplitude (20). However, Cl^- secretion was missing in $TMEM16A^{-/-}$ animals (Fig. 1, *A* and *B*). Cl^- secretion in wt animals was followed by a transient K^+ secretion (positive voltage deflection) that was present in both +/+ and −/− animals (Fig. 1*A*). Thus Ca^{2+}-dependent

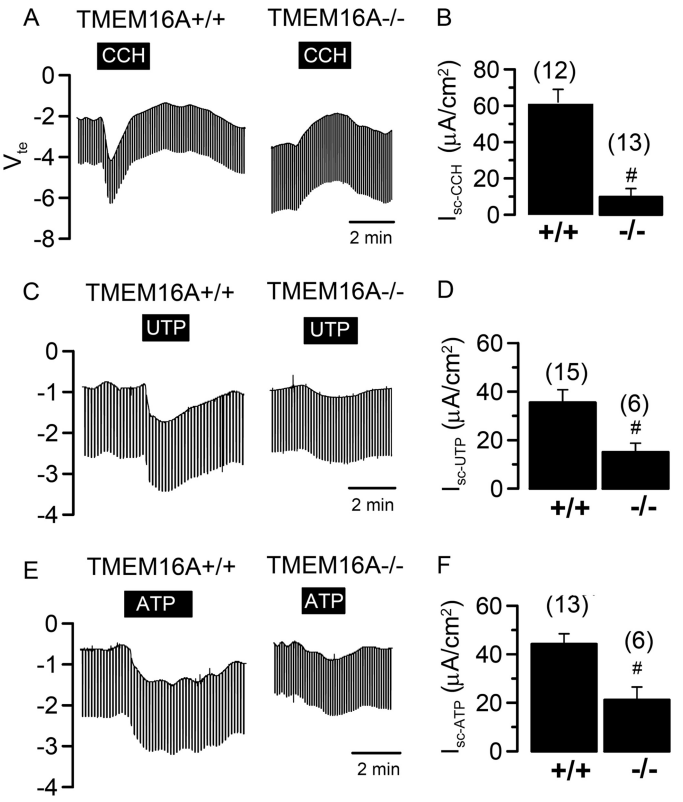

FIGURE 1. **Defective Ca^{2+}-dependent Cl^- secretion in airways of $TMEM16A^{-/-}$ animals.** *A*, Ussing chamber recording of the transepithelial voltage (V_{te}) in isolated mouse trachea. CCH (100 μM) activated a transient lumen negative V_{te} in tracheas of $TMEM16A^{+/+}$ animals indicating activation of Ca^{2+}-dependent Cl^- secretion. Ca^{2+}-dependent Cl^- secretion was missing in tracheas of $TMEM16A^{-/-}$ mice. *B*, summary of the equivalent short circuit currents (I_{sc}) indicates largely reduced cholinergic Cl^- secretion in $TMEM16A^{-/-}$ tracheas. *C* and *D*, activation of lumen negative V_{te} and short circuit currents by luminal application of 100 μM UTP in tracheas of $TMEM16A^{+/+}$ mice, which were reduced in $TMEM16A^{-/-}$ tracheas. *E* and *F*, activation of lumen negative V_{te} and short circuit currents by luminal application of 100 μM ATP in tracheas of $TMEM16A^{+/+}$ mice, which were reduced in $TMEM16A^{-/-}$ tracheas. Mean ± S.E. (n = number of tissues measured). #, significant difference when compared with $TMEM16A^{+/+}$. Mean ± S.E. (n = number of tissues measured). *, significant effect of CCH (paired t test). #, significant difference when compared with $TMEM16A^{+/+}$.

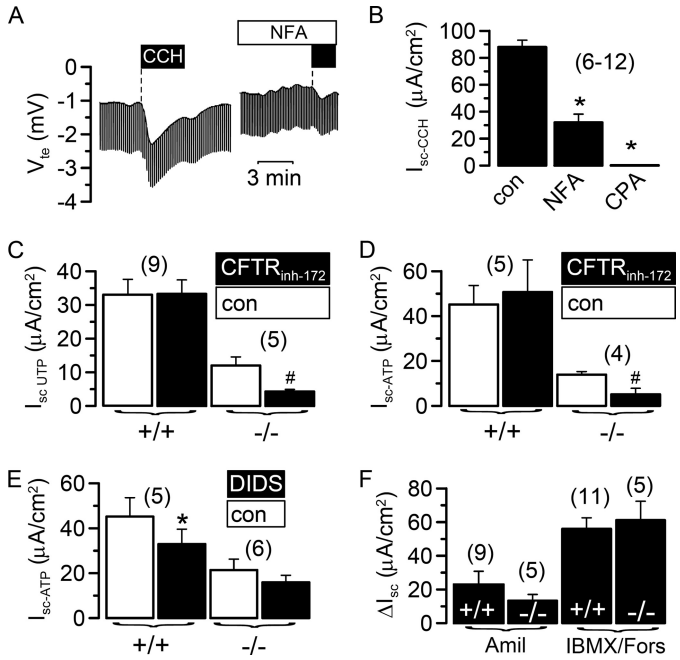

FIGURE 2. **Residual chloride secretion in TMEM16A$^{-/-}$ airways is due to CFTR.** *A*, transepithelial voltage and effect of carbachol (100 μM, *black bar*) measured in a trachea of a TMEM16A$^{+/+}$ mouse in the absence and presence of niflumic acid (*NFA*, 100 μM). *B*, summary of the equivalent short circuit currents (I_{sc}) indicates inhibition of cholinergic Cl^- secretion in TMEM16A$^{+/+}$ tracheas by niflumic acid and cyclopiazonic acid (*CPA*; 100 μM). *C* and *D*, effect of the CFTR inhibitor CFTRinh-172 (5 μM) on UTP- and ATP-activated Cl^- secretion in tracheas of TMEM16A$^{+/+}$ and TMEM16A$^{-/-}$ animals. ATP-activated Cl^- currents are largely reduced in −/− tracheas. Residual Cl^- secretion is inhibited significantly by the CFTRinh-172. *E*, ATP-activated Cl^- secretion is inhibited by DIDS (100 μM) in tracheas of TMEM16A$^{+/+}$ but not TMEM16A$^{-/-}$ animals. *F*, amiloride (*Amil*)-sensitive Na^+ absorption and CFTR-dependent Cl^- secretion activated by isobutylmethylxanthine (*IBMX*; 100 μM) and forskolin (*Fors*; 2 μM) were not different between TMEM16A$^{+/+}$ and TMEM16A$^{-/-}$ tracheas. Mean ± S.E. (*n* = number of tissues measured). *, significant effects of inhibitors (paired *t* test). #, significant difference when compared with TMEM16A$^{-/-}$. *con*, control.

Cl^- secretion was almost absent in TMEM16A$^{-/-}$ animals, whereas K^+ secretion was unaffected. Stimulation of apical purinergic receptors by UTP increased a transient Cl^- secretion in +/+ tracheas but had only small effects on −/− tracheas (Fig. 1, C and *D*). A similar phenotype was observed when $P2Y_2$ receptors were stimulated with ATP (Fig. 1, *E* and *F*).

The small increase in Cl^- secretion by purinergic stimulation of −/− tracheas is probably due to activation of CFTR (21), as the specific inhibitor CFTRinh-172 inhibited the remaining short circuit current (I_{sc}) (Fig. 2, *C* and *D*). Moreover, other members of the TMEM16 family of proteins are expressed in mouse trachea, which may also contribute to the remaining Ca^{2+}-activated Cl^- conductance (17). In contrast to CFTRinh-172, the TMEM16A inhibitor DIDS inhibited Cl^- transport only in wt animals (Fig. 2*E*). Moreover, unlike Ca^{2+}-activated Cl^- channels, amiloride-sensitive Na^+ absorption and CFTR-dependent Cl^- secretion were not disturbed in TMEM16A-null mice (Fig. 2*F*).

TMEM16A Is Important for Mucociliary Clearance in Murine Trachea—Attenuated Cl^- secretion in neonatal tracheas could be due to low levels of expression of TMEM16A. In fact, *in situ* hybridization showed very little signal in the surface epithelium of neonatal trachea, whereas expression was clearly detectable in cells of the submucosal glands (Fig. 3*A*). No signal was obtained for the sense probe. Submucosal cells appear to be the major target for cholinergic stimulation of airway secretion (22). As mucociliary transport in the airways depends on cholinergic Cl^- secretion, we examined transport of black polystyrene microspheres on freshly isolated tracheas in a humidified chamber, as a measure for mucociliary transport. Mucociliary particle transport was activated in +/+ tracheas by stimulation with CCH, and was inhibited by the TMEM16A inhibitor DIDS (Fig. 3*B*-D). In contrast, neither cholinergic stimulation nor the TMEM16A inhibitor DIDS had any effects on particle transport observed in −/− tracheas, indicating lack of cholinergic mucociliary clearance in TMEM16A$^{-/-}$ mice. Moreover, as neonatal mouse tracheas show relatively small effects of purinergic agonists (ATP and UTP) on Cl^- secretion (Fig. 1, *C*–*F*), stimulation by ATP had little effects on particle transport in airways of both +/+ and −/− (supplemental Fig. 1*A*).

Lack of cholinergically stimulated clearance may contribute to the high lethality of 16a-null mice. These results suggest TMEM16A as an important factor for the control of mucociliary clearance in human airways as suggested in a previous report (17). Using a specific anti-human TMEM16A antibody, we detected expression of TMEM16A in surface epithelial cells as well as the serous parts of submucosal glands of human airways (Fig. 4, *A* and *C*), while mucous tubules were free of human TMEM16A expression (Fig. 4*E*). No staining was seen in the absence of the primary antibody (Fig. 4, *B*, *D*, and *F*). Notably, most of the TMEM16A seemed to be localized intracellularly, and only a small fraction appears in the cell membrane. When we examined TMEM16A in mouse airways, a similar distribution was found (supplemental Fig. 1). TMEM16A has also been found earlier in both intracellular compartments and plasma membrane in interstitial cells of Cajal (23), gastrointestinal stromal tumors (24), as well as various epithelial organs, including trachea (14). In contrast, TMEM16A overexpressed in HEK293 cells appears clearly membrane-localized (supplemental Fig. 2*B*). This discrepancy currently remains unexplained.

Ca^{2+}-dependent Cl^- Secretion Is Defective in Mouse Colon of TMEM16A-null Mice—Cl^- transport can also be activated by Ca^{2+} in the neonatal colon, which has been shown to play an important role during rotavirus-induced diarrhea (25). We found that stimulation of the neonatal +/+ colon with carbachol activated a transient Cl^- secretion that was not detectable in the colon of TMEM16A$^{-/-}$ animals (Fig. 5, *A* and *B*). In contrast, CFTR-dependent Cl^- secretion and amiloride-sensitive Na^+ absorption were indistinguishable between wt and knock-out animals (Fig. 5*C*). Thus, TMEM16A is crucial for Ca^{2+}-induced Cl^- transport in the neonatal colon (26).

Defective Ca^{2+}-dependent Cl^- Secretion in Pancreatic Acinar Cells of TMEM16A-null Mice—Archetypical tissues for Ca^{2+}-dependent Cl^- secretion are glands of gastrointestinal organs (2). Ca^{2+}-dependent Cl^- channels are important for production of saliva and pancreatic juice. Ca^{2+}-dependent stimulation of salivary and pancreatic glands activates both Cl^- and K^+ channels (5, 6, 27). Expression of TMEM16A in mouse salivary, pancreatic, and mammary gland has been reported recently (14, 15). However, although real time reverse transcription-PCR analysis of TMEM16A clearly showed expres-

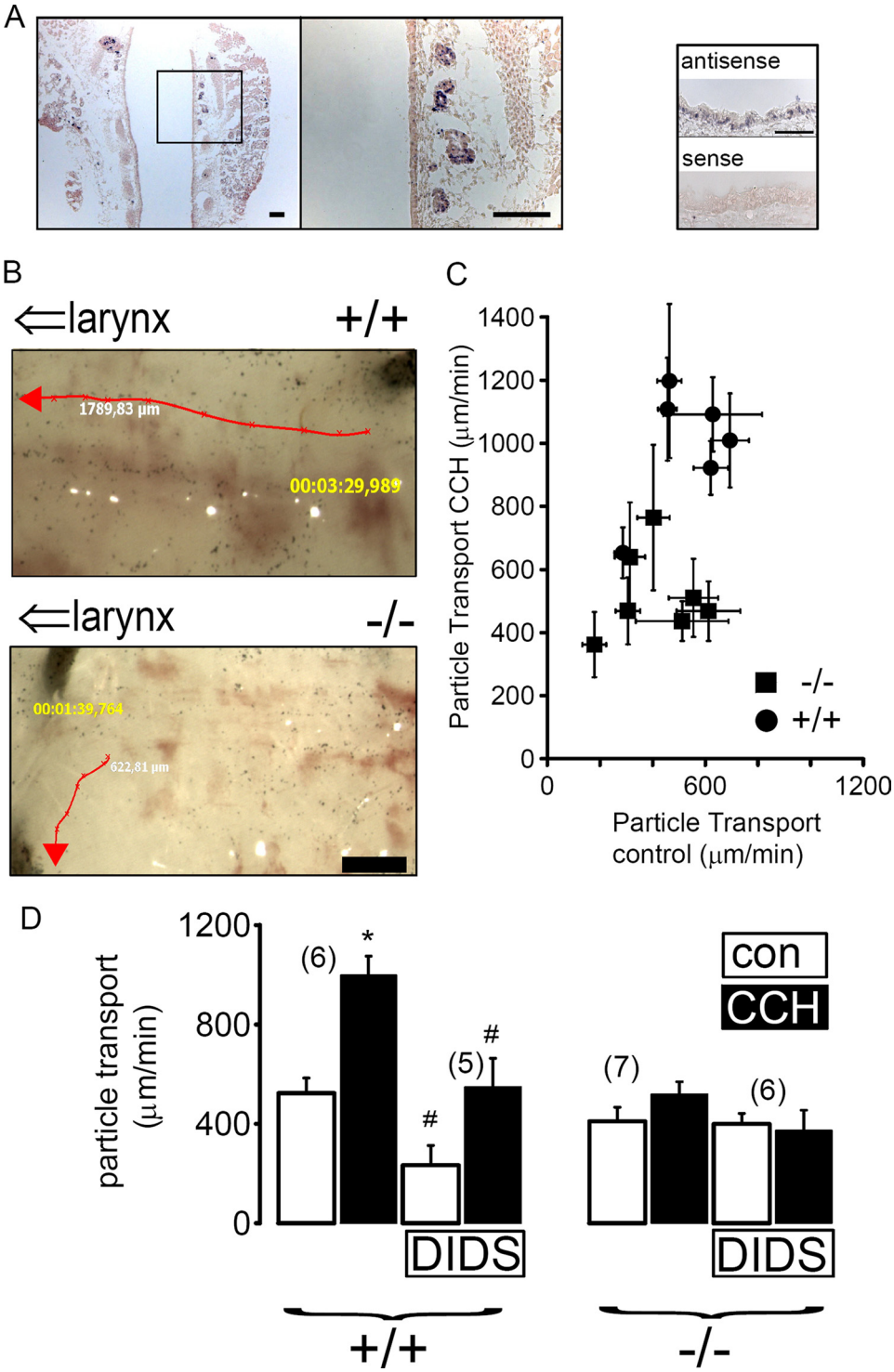

FIGURE 3. **Lack of cholinergic airway gland secretion compromises mucociliary clearance.** *A*, *in situ* hybridization of TMEM16A in neonatal TMEM16A$^{+/+}$ trachea. mRNA for TMEM16A was expressed at low levels in the surface epithelium (*left panel*) but was detectable in submucosal glands (*left panel*). *Scale bar*, 200 μm. No signal was detected by hybridization with a sense probe (*right panel*; *scale bar*, 50 μm). *B*, tracking of black polystyrene microsphere movement on the surface of a neonatal TMEM16A$^{+/+}$ trachea in a humidified chamber before and after stimulation with CCH (100 μM). *C*, diagram showing particle transport under control conditions and increase after stimulation with CCH. *Scale bar*, 1 mm. *D*, summary of particle transport on tracheas of wt (+/+) and TMEM16A$^{-/-}$ animals. Particle transport in −/− tracheas was neither increased by cholinergic stimulation with carbachol (100 μM) nor inhibited by DIDS (100 μM). Mean ± S.E. (n = number of tissues measured). *, significant effect of CCH (paired t test). #, significant difference when compared with TMEM16A$^{-/-}$.

sion in adult mouse pancreas (data not shown), we were unable to detect TMEM16A in the neonatal pancreas by immunohistochemistry, suggesting low levels of expression, similar to the neonatal airways (supplemental Fig. 2*A*).

Nonetheless, in whole-cell patch clamp experiments with freshly isolated pancreatic acini from wt animals, we found rapid and transient activation of a whole-cell conductance by cholinergic stimulation with carbachol (Fig. 6, *A*–*C*). As observed in previous reports on endogenous Ca^{2+}-activated Cl^- currents (reviewed in (2) and as reported for TMEM16A (14), initial (10 s after CCH application) currents were strongly outwardly rectifying but then linearized (30 s after CCH application), probably due to a further increase in intracellular Ca^{2+} (Fig. 6*D*). Moreover, activation of time-dependent whole-cell currents was only observed in cells from TMEM16A$^{+/+}$ animals but not in cells from TMEM16A-null mice (Fig. 6*E*). Carbachol stimulation of acinar cells from TMEM16A$^{-/-}$ animals induced only small whole-cell currents (Fig. 6, *A*–*C*). Activation of whole-cell conductance and depolarization of the membrane voltage (V_m) due to opening of Ca^{2+}-dependent Cl^- channels was largely reduced and missing, respectively, in pancreatic acinar cells from TMEM16A$^{-/-}$ mice (Fig. 6*C*).

Defective Ca^{2+}-dependent Cl^- Secretion in Hepatocytes and Salivary Acinar Cells of TMEM16A-null Mice—Ca^{2+}-activated Cl^- channels have also been observed previously in hepatocytes (28, 29). In freshly isolated TMEM16A$^{+/+}$ hepatocytes, a small but clearly detectable whole-cell current was activated by carbachol (Fig. 7*A*). In contrast, hepatocytes of TMEM16A$^{-/-}$ mice lacked Ca^{2+}-dependent whole cell conductance (Fig. 7, *A* and *B*). Moreover, Ca^{2+}-dependent whole-cell conductance in +/+ cells was largely inhibited by the TMEM16A blocker DIDS, whereas DIDS had no effect on −/−

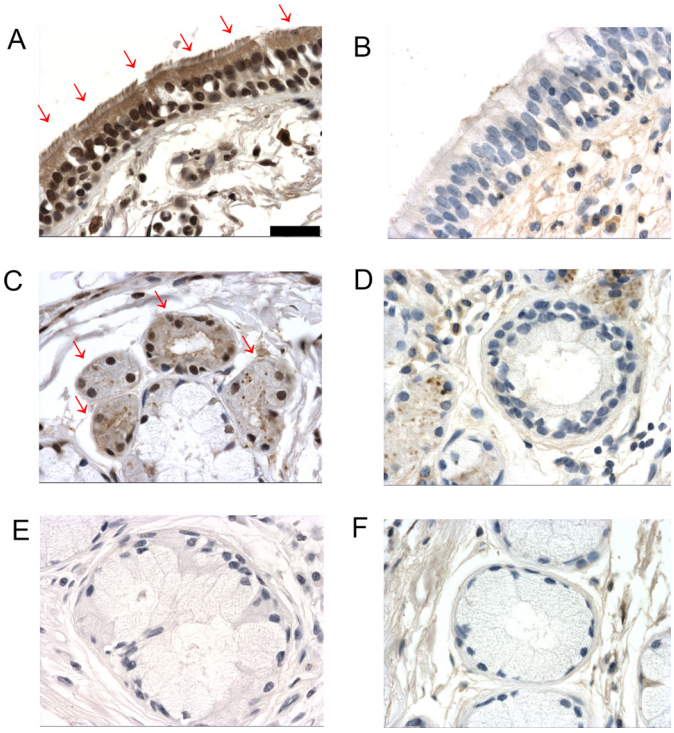

FIGURE 4. **Expression of TMEM16A in human airways.** *A*, expression of TMEM16A in the surface epithelium of a mid-size bronchus. *C*, expression of TMEM16A in serous end pieces of submucosal glands. *E*, lack of TMEM16A expression in larger mucous ducts. Most staining was detected close to the apical membrane and intracellular compartment. *B*, *D*, and *F*, negative controls in the absence of a primary antibody. *Scale bar*, 20 μm. *Arrows* indicate apical staining for TMEM16A.

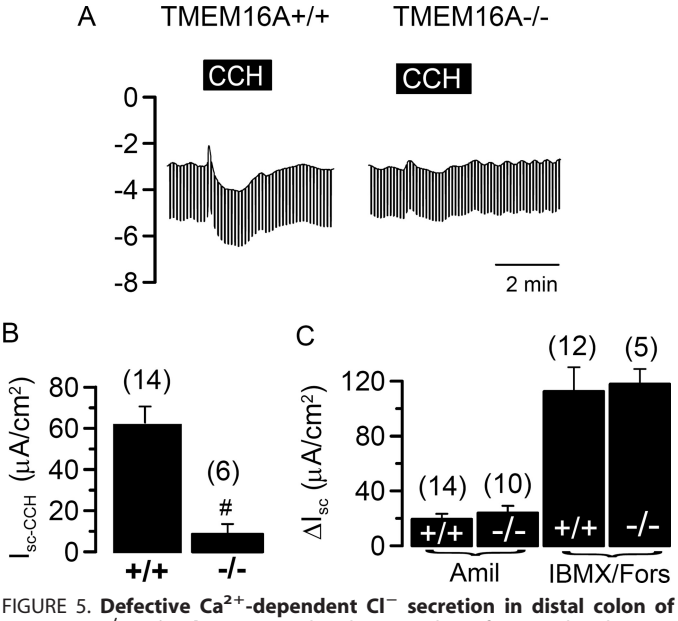

FIGURE 5. **Defective Ca^{2+}-dependent Cl^- secretion in distal colon of TMEM16A$^{-/-}$ animals.** *A*, Ussing chamber recording of V_{te} in isolated mouse colon from wt and TMEM16A-null mice. CCH (100 μM) activated a transient lumen negative V_{te} in colon of TMEM16A$^{+/+}$ animals, indicating activation of Ca^{2+}-dependent Cl^- secretion, which was missing in tracheas of TMEM16A$^{-/-}$ mice. *B*, summary of the equivalent short circuit currents indicates largely reduced cholinergic Cl^- secretion in TMEM16A$^{-/-}$ colon. *C*, amiloride (*Amil*)-sensitive Na^+ absorption and CFTR-dependent Cl^- secretion activated by isobutylmethylxanthine (*IBMX*; 100 μM) and forskolin (*Fors*; 2 μM) were not different in colon from TMEM16A$^{+/+}$ and TMEM16A$^{-/-}$ mice. Mean ± S.E. (n = number of cells or tissues measured). #, significant difference when compared with TMEM16A$^{-/-}$.

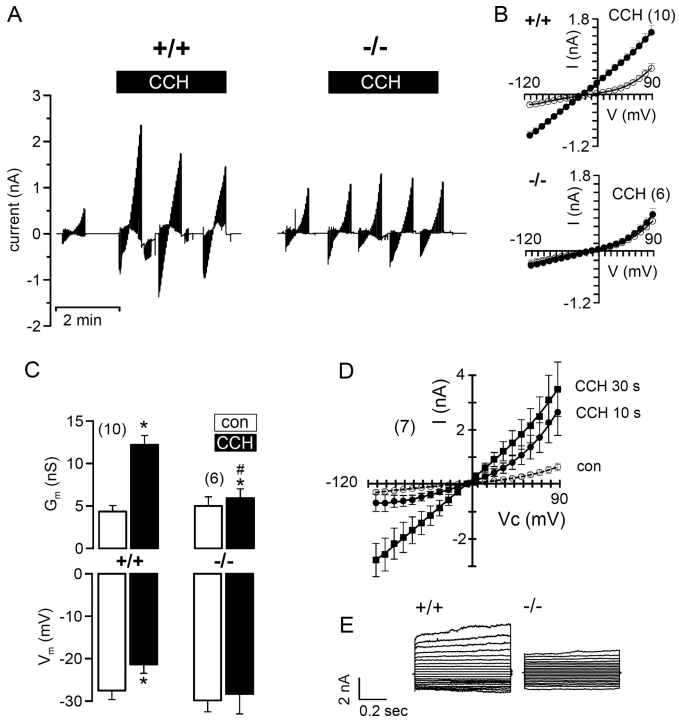

FIGURE 6. **Defective cholinergic Cl^- secretion in pancreatic acinar cells of TMEM16A$^{-/-}$ animals.** *A*, continuous recordings of the whole-cell current measured in pancreatic acinar cells at a clamp voltage range of −110 to + 90 mV. CCH (100 μM) activated a large whole-cell current in acinar cells from TMEM16a$^{+/+}$ animals that was greatly reduced in cells from TMEM16A-null mice (−/−). *B*, summary *I/V* curves obtained under control conditions and after stimulation with CCH of +/+ and −/− cells indicating lack of Ca^{2+}-activated Cl^- currents in cells from TMEM16A-null mice. *C*, summary of calculated whole-cell conductances (G_m) and membrane voltages (V_m) and effect of CCH, indicating reduced Ca^{2+}-activated Cl^- conductances in cells from TMEM16A-null mice. *D* and *E*, I/V curves and currents recordings obtained in whole-cell patch clamp experiments with NaCl as pipette filling solution. CCH-induced currents were initially (after 10 s) outwardly rectifying but then changed to more linear currents (30 s). Time-dependent whole-cell currents after CCH stimulation were only detected in TMEM16A$^{+/+}$ cells. Mean ± S.E. (n = number of cells measured). *, significant effect of CCH (paired t test). #, significant difference when compared with TMEM16A$^{-/-}$.

hepatocytes (Fig. 7, *A* and *B*). We noticed the strong inhibitory effect of DIDS on whole-cell currents in hepatocytes, which has also been observed earlier (29). It is well known that Ca^{2+}-activated Cl^- currents in different tissues have different sensitivity toward pharmacological inhibitors such as DIDS (reviewed in (2). We may speculate that other endogenous TMEM16 channels coexpressed differentially in different organs, may determine the pharmacological profile of Ca^{2+}-activated Cl^- currents.

Similar to pancreatic acinar cells, salivary glands also express TMEM16A (14, 15). In this tissue, however, activation of Ca^{2+}-dependent K^+ channels dominates (6). Carbachol-induced whole-cell conductances in submandibular acinar cells from TMEM16A$^{+/+}$ and TMEM16A$^{-/-}$ mice were indistinguishable in size (Fig. 7*C*). We noticed that the membrane voltage (V_m) of TMEM16A$^{-/-}$ cells was more hyperpolarized under resting conditions (−61 ± 4.5 mV; n = 6) when compared with TMEM16A$^{+/+}$ cells (−48 ± 4.7 mV; n = 9). Moreover, CCH depolarized V_m of TMEM16A$^{+/+}$ cells (by 8.3 ± 1.6 mV) but hyperpolarized V_m of TMEM16A$^{-/-}$ cells (by 12.1 ± 2.7 mV) (Fig. 7, *D* and *E*). Notably, activation of whole cell conductance

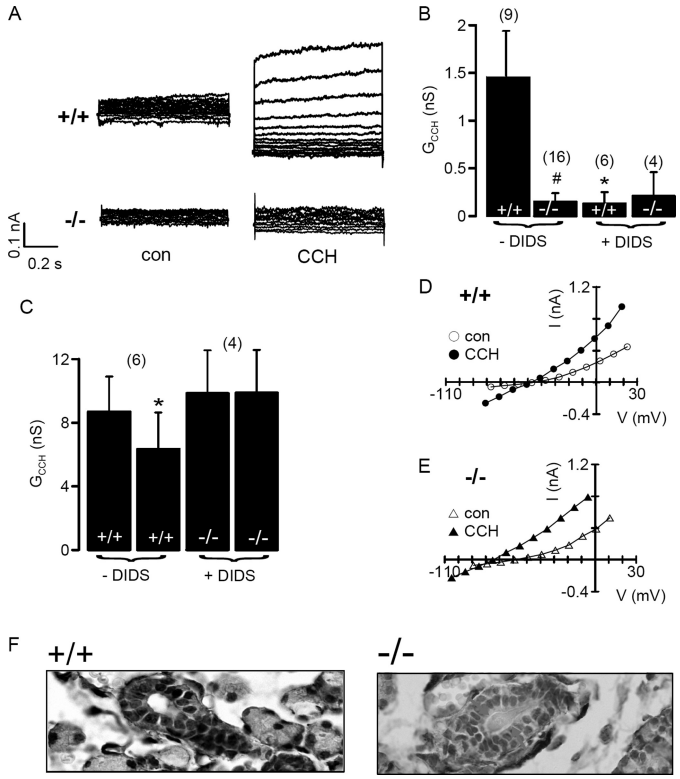

FIGURE 7. **Defective cholinergic Cl^- secretion in hepatocytes and submandibular acinar cells of TMEM16A$^{-/-}$ animals.** *A*, whole-cell currents measured in freshly isolated hepatocytes from wt and TMEM16A-null mice under control conditions and after stimulation with CCH. *B*, summary of carbachol-induced whole-cell conductance shows lack of activation of conductance in TMEM16A-null cells. DIDS inhibited whole-cell conductances only in wt cells. *C*, summary of carbachol-induced whole-cell conductances and effect of DIDS in freshly isolated submandibular acinus cells from TMEM16A$^{+/+}$ and TMEM16A-null mice. *D* and *E*, current/voltage relationships obtained in submandibular acinus cells before and after stimulation with carbachol (100 μM), indicating a hyperpolarized membrane voltage in cells from TMEM16A-null mice. *F*, TMEM16A was detected in +/+ but not −/− submandibular glands. Glands from TMEM16A$^{-/-}$ mice appeared enlarged and were filled with mucus. Mean ± S.E. (*n* = number of cells measured). *, significant effect of CCH (paired *t* test). #, significant difference when compared with TMEM16A$^{-/-}$.

by CCH was inhibited by DIDS only in TMEM16A$^{+/+}$ cells, suggesting a contribution of Cl^- channels to Ca^{2+}-dependent secretion in submandibular acinar cells (Fig. 7*C*). Moreover, in the absence of Cl^- in the bath (5 mM Cl^-), stimulation of +/+ cells by CCH no longer depolarized but hyperpolarized the membrane voltage, similar to −/− cells (data not shown). Finally, TMEM16A was detected in +/+ but not −/− glands, which, in the case of TMEM16A$^{-/-}$, appeared enlarged and filled by mucous (Fig. 7*F*). We therefore suggest a dysfunction of salivary glands in TMEM16A$^{-/-}$ mice, as suggested previously (14). Taken together, the present results demonstrate the importance of TMEM16A for Ca^{2+}-dependent Cl^- transport in a number of epithelial tissues. This knowledge may provide the basis for novel pharmacological strategies for the treatment of cystic fibrosis, because Ca^{2+}-dependent Cl^- channels may be activated to compensate for defective CFTR Cl^- channel function (30, 31). Because TMEM16A is also important for Ca^{2+}-dependent Cl^- transport in the intestine and salivary glands, the current results may also be relevant for infectious secretory diarrhea and Sjögren syndrome (6).

REFERENCES

1. Riordan, J. R., Rommens, J. M., Kerem, B., Alon, N., Rozmahel, R., Grzelczak, Z., Zielenski, J., Lok, S., Plavsic, N., and Chou, J. L. (1989) *Science* **245,** 1066–1073
2. Hartzell, C., Putzier, I., and Arreola, J. (2005) *Annu. Rev. Physiol.* **67,** 719–758
3. Kunzelmann, K., Milenkovic, V. M., Spitzner, M., Soria, R. B., and Schreiber, R. (2007) *Pflugers Arch.* **454,** 879–889
4. Jentsch, T. J., Stein, V., Weinreich, F., and Zdebik, A. A. (2002) *Physiol. Rev.* **82,** 503–568
5. Petersen, O. H., and Tepikin, A. V. (2008) *Annu. Rev. Physiol.* **70,** 273–299
6. Melvin, J. E., Yule, D., Shuttleworth, T., and Begenisich, T. (2005) *Annu. Rev. Physiol.* **67,** 445–469
7. Sato, K., and Sato, F. (1984) *J. Clin. Invest.* **73,** 1763–1771
8. Choi, J. Y., Joo, N. S., Krouse, M. E., Wu, J. V., Robbins, R. C., Ianowski, J. P., Hanrahan, J. W., and Wine, J. J. (2007) *J. Clin. Invest.* **117,** 3118–3127
9. Boucher, R. C. (2003) *Pflugers Arch.* **445,** 495–498
10. Hartzell, H. C., Qu, Z., Yu, K., Xiao, Q., and Chien, L. T. (2008) *Physiol. Rev.* **88,** 639–672
11. Barro-Soria, R., Spitzner, M., Schreiber, R., and Kunzelmann, K. (September 26, 2006) *J. Biol. Chem.* 10.1074/jbc.M605716200
12. Barro-Soria, R., Schreiber, R., and Kunzelmann, K. (2008) *Biochim. Biophys. Acta* **1783,** 1993–2000
13. Milenkovic, V. M., Soria, R. B., Aldehni, F., Schreiber, R., and Kunzelmann, K. (2009) *Pflugers Arch.* **458,** 431–441
14. Yang, Y. D., Cho, H., Koo, J. Y., Tak, M. H., Cho, Y., Shim, W. S., Park, S. P., Lee, J., Lee, B., Kim, B. M., Raouf, R., Shin, Y. K., and Oh, U. (2008) *Nature* **455,** 1210–1215
15. Schroeder, B. C., Cheng, T., Jan, Y. N., and Jan, L. Y. (2008) *Cell* **134,** 1019–1029
16. Caputo, A., Caci, E., Ferrera, L., Pedemonte, N., Barsanti, C., Sondo, E., Pfeffer, U., Ravazzolo, R., Zegarra-Moran, O., and Galietta, L. J. (2008) *Science* **322,** 590–594
17. Rock, J. R., O'Neal, W. K., Gabriel, S. E., Randell, S. H., Harfe, B. D., Boucher, R. C., and Grubb, B. R. (2009) *J. Biol. Chem.* **284,** 14875–14880
18. Rock, J. R., Futtner, C. R., and Harfe, B. D. (2008) *Dev. Biol.* **321,** 141–149
19. Greger, R., and Kunzelmann, K. (1991) *Pflugers Arch.* **419,** 209–211
20. Kunzelmann, K., Schreiber, R., and Cook, D. I. (2002) *Pflugers Arch.* **444,** 220–226
21. Faria, D., Schreiber, R., and Kunzelmann, K. (2009) *Pflugers Arch.* **457,** 1373–1380
22. Wine, J. J. (2007) *Auton. Neurosci.* **133,** 35–54
23. Gomez-Pinilla, P. J., Gibbons, S. J., Bardsley, M. R., Lorincz, A., Pozo, M. J., Pasricha, P. J., van de, R. M., West, R. B., Sarr, M. G., Kendrick, M. L., Cima, R. R., Dozois, E. J., Larson, D. W., Ordog, T., and Farrugia, G. (2009). *Am. J. Physiol. Gastrointest. Liver Physiol.* **296,** G1370–1381
24. Espinosa, I., Lee, C. H., Kim, M. K., Rouse, B. T., Subramanian, S., Montgomery, K., Varma, S., Corless, C. L., Heinrich, M. C., Smith, K. S., Wang, Z., Rubin, B., Nielsen, T. O., Seitz, R. S., Ross, D. T., West, R. B., Cleary, M. L., and van de Rijn, R. M. (2008) *Am J. Surg. Pathol.* **32,** 210–218
25. Ball, J. M., Tian, P., Zeng, C. Q., Morris, A. P., and Estes, M. K. (1996) *Science* **272,** 101–104
26. Morris, A. P., Scott, J. K., Ball, J. M., Zeng, C. Q., O'Neal, W. K., and Estes, M. K. (1999) *Am. J. Physiol.* **277,** G431–G444
27. Petersen, O. H. (1986) *Am. J. Physiol.* **251,** G1–13
28. Aromataris, E. C., Roberts, M. L., Barritt, G. J., and Rychkov, G. Y. (2006) *J. Physiol.* **573,** 611–625
29. Koumi, S., Sato, R., and Aramaki, T. (1994) *J. Gen. Physiol.* **104,** 357–373
30. Kunzelmann, K. (1999) *Rev. Physiol. Biochem. Pharmacol.* **137,** 1–70
31. Kuruma, A., and Hartzell, H. C. (2000) *J. Gen. Physiol* **115,** 59–80